BIOCHEMISTRY
including biophysical chemistry & molecular biology

ARTICLE

pubs.acs.org/biochemistry

Mechanism of Androgen Receptor Antagonism by Bicalutamide in the Treatment of Prostate Cancer

D. J. Osguthorpe[§] and A. T. Hagler[*,§,†,‡]

[†]Department of Chemistry and Department of Biochemistry and Molecular Biology, University of Massachusetts, 701 Lederle Graduate Research Tower, 710 North Pleasant Street, Amherst, Massachusetts 01003-9336, United States

[‡]Department of Pharmaceutical Chemistry, University of California San Francisco, 600 16th Street, San Francisco, California 94158-2517, United States

[§]Shifa Biomedical, 1 Great Valley Parkway, Suite 8, Malvern, Pennsylvania 19355, United States

ABSTRACT: The androgen receptor (AR) plays a key role in regulating gene expression in a variety of tissues, including the prostate. In that role, it is one of the primary targets in the development of new chemotherapeutics for treatment of prostate cancer and the target of the most widely prescribed current drug, bicalutamide (Bcu), for this disease. In view of its importance, and the absence of a crystal structure for any antagonist−AR complex, we have conducted a series of molecular dynamics-based simulations of the AR−Bcu complex and quantum mechanical (QM) calculations of Bcu, to elucidate the structural basis for antagonism of this key target. The structures that emerge show that bicalutamide antagonizes AR by accessing an additional binding pocket (B-site) adjacent to the hormone binding site (HBS), induced by displacing helix 12. This distorts the coactivator binding site and results in the inactivation of transcription. An alternative equienergetic conformational state of bicalutamide was found to bind in an expanded hormone pocket without materially perturbing either helix 12 or the coactivator binding site. Thus, both the structural basis of antagonism and the mechanism underlying agonist properties displayed by bicalutamide in different environments may be rationalized in terms of these structures. In addition, the antagonist structure and especially the induced second site (B-site) provide a structural framework for the design of novel antiandrogens.

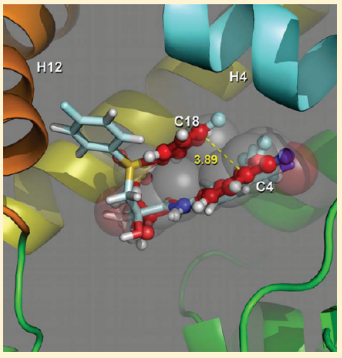

The androgen receptor (AR) is a nuclear receptor (NR)[1,2] that responds to the hormones testosterone (T) and dihydrotestosterone (DHT) by modulating gene expression in a variety of cells, including prostate and muscle tissue. The androgen-activated receptor enters the nucleus and anchors the assembly of a large complex of transcription factors at target promoters and enhancers. Some 40 years ago, Huggins noted that prostate cancers (PC) require androgen for growth.[3] On the basis of this observation, androgen ablation therapy and/or antiandrogens such as Casodex (bicalutamide) are the primary approaches to treating PC.[4] Unfortunately, after being treated for 2−3 years, the cancer evolves to an "androgen-independent" or hormone refractory state, and current antiandrogens become ineffective.[5]

The ligand binding domain (LBD) is the heart of the receptor and has been the focus of AR-based drug discovery. Crystal structures of the AR LBD containing numerous bound ligands and coactivator peptides have been determined.[6−10] When the hormone binds to the hormone binding site (HBS), an uncharacterized reorganization of the receptor occurs, primarily thought to be the registration of helix 12 (H12) to bind the coactivator. This reorganization results in the formation of an effective coactivator binding site (AF-2 site), a surface-exposed HΦ cleft involving helices H3, H4, and H12 (Figure 1).

The precise mechanism by which AR antagonists block the transcription of target genes remains elusive. The preponderance of evidence from X-ray structures of several NR−antagonist complexes suggests that the general mechanism involves perturbing helix 12, displacing it from its hormone-bound configuration, and distorting the AF-2 site.[1,2] This in turn interferes with coactivator binding, a requisite for transcription. Although indubitably this is the case in the AR as well, to date native AR in its antagonized state, i.e., a wild-type (WT) AR−antagonist complex, has defied crystallization. Thus, no structural information about the nature of the antagonist-induced structural change exists. Perhaps even more of a mystery is how overexpression of AR or stimulation by cytokine IL1-β, implicated in the transition to the androgen-independent state, causes bicalutamide (Figure 2) and other antagonists to become agonists.[11−13]

To understand the molecular interactions underlying AR antagonism, we have exploited in silico simulations, including molecular dynamics (MD), quantum mechanics (QM), and a "slow growth" technique employing free energy perturbation theory (FEP), of the AR−Bcu complex to explore the binding modes accessible to Bcu in the AR LBD. MD has recently been used in an analogous way to determine the effects of ligand binding on the coactivator affinity of nuclear receptor LRH-1.[14] Similarly, Zhou

Received: December 26, 2010
Revised: March 24, 2011
Published: April 05, 2011

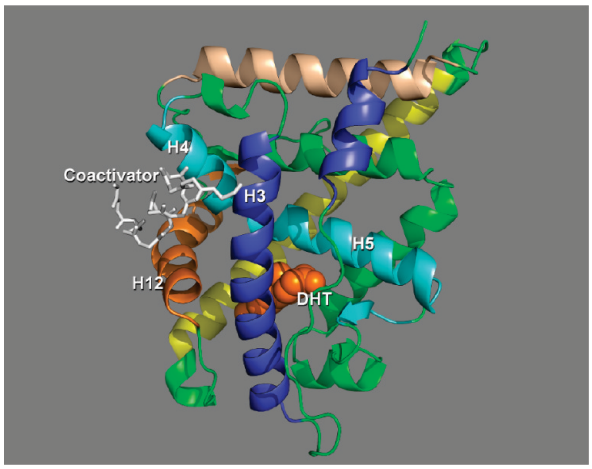

Figure 1. AR LBD with DHT (orange space-filling diagram) and coactivator peptide (white sticks) shown. Binding of DHT at the HBS organizes H12 that, along with H3 and H4, forms the AF-2 site allowing coactivators to bind (Estebanez-Perpina et al., Protein Data Bank entry 1T63).

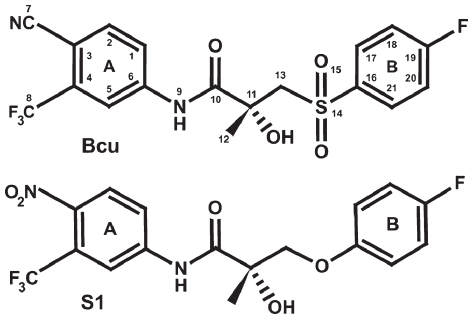

Figure 2. Schematic of bicalutamide (Bcu) and S1.

et al. have conducted computational studies of hydroxyflutamide binding to the wild-type AR and the T877A mutant,[15] and these studies suggest that the transition from an antagonist to an agonist in the latter system corresponds to H12 adopting an agonist conformation, consistent with the importance of conformational changes in H12 to the mechanism of antagonism in the wild-type AR. Other MD studies of the AR have looked at the effect of pathogenic mutations to the AR that led to androgen insensitivity syndrome,[16] where mutations in the receptor were shown computationally to cause changes in the ligand binding site that lead to an inactive AR.[17,18] We seek to understand the structural basis for the pharmacological activity of this drug and, if possible, to gain insight into the molecular mechanisms underlying conversion of antagonists into agonists. In addition, although the use of structure−activity relationships (SARs) has proven to be very successful in developing new clinical candidates of antiandrogens,[19−23] not all patients respond to these second-generation antagonists and resistance still emerges,[20] and thus, third-generation antiandrogens are required. The elucidation of the antagonist-bound structure should provide a better basis for us and others to exploit structure-based design in the development of more potent and effective therapeutics, especially compounds that overcome androgen-independent or refractory PC.[5]

MATERIALS AND METHODS

The first step in the MD simulations involves building the system. The 1T63 structure of the AR bound to DHT and a coactivator peptide (Figure 1) from the Fletterick lab was used as the basis for all simulations.[9] Missing atoms and hydrogens were built in. Two different initial structures of the Bcu−AR complex were constructed, exploiting the AR W741L−Bcu and AR−S1 complexes as a basis for initial ligand placement. A third, independent trajectory was followed by the FEP-slow growth method, also described below. For comparison and as a test of the simulation method, the experimentally determined AR complexes with DHT and the mutant W741L AR with Bcu were also simulated.

Initial Structure of WT AR−Bcu Complexes. As noted above, no structure of Bcu bound to the wild-type receptor has been determined. However, a mutant AR, W741L, arose in the LNCaP prostate cancer cell line upon androgen depletion and treatment with bicalutamide. At first, these cells did not grow, but after 6−13 weeks, Bcu stimulated cell growth (rather than antagonizing it). Transactivation assays confirmed that mutation of W741 to Leu converts Bcu into an agonist,[24] and this complex has been crystallized and its structure determined.[25] Although this AR mutation, in complex with Bcu, results in an agonist conformation of the receptor (presumably the reason it could be crystallized), we exploited the Bcu configuration in this complex by superposing it onto the 1T63 structure from the Fletterick lab[9] and used the resulting Bcu coordinates in the HBS (hormone binding site) of 1T63. Not surprisingly, Bcu clashes sterically with W741 in this construct. To address this, we slightly shifted both the B-ring of Bcu (Figure 2) and W741 to relieve the overlap prior to equilibration.

To overcome bias or artifacts introduced by a single set of initial conditions and a single run, we also simulated a system starting from Bcu in the structure of AR with agonist S1.[26] S1 differs from Bcu only in the replacement of the sulfonyl group with an ether linkage and the replacement of the cyano group in the para position of the A-ring with NO_2 (Figure 2), yet it is an agonist and stabilizes the agonist conformation of AR.[26] To build this construct, key side chains in the 1T63 HBS, especially W741, M745, and M895, were positioned in their configurations in the S1−AR complex and Bcu was inserted into the resulting S1 configuration.

Force Field, Ligand Charges, and Torsional Barriers. Simulations were conducted with the OPLS all-atom potential for the AR, as implemented in GROMACS.[27] Although potentials for proteins have been well characterized for many years,[28,29] this is not the case for arbitrary heterocyclic ligands such as Bcu. Fortunately, OPLS had bond stretching and angle bending parameters for the functional groups found in DHT and S1. QM calculations of the more critical rotational barriers of each ligand were conducted, and torsion parameters generated to fit these barriers were used. Partial atomic charges on the ligand were determined by QM. These calculations were performed using DFT at the 6-31G** level with the Jaguar package (Schrödinger).

System Setup and Equilibration. The AR−ligand complexes were solvated with ∼10000 water molecules in a dodecahedral box extending 6 Å around the receptor, using genbox (Gromacs). In addition, five chloride counterions were added to neutralize the system (using Genion). The solvated system was then minimized, with heavy atoms restrained to reorient hydrogen atoms. Following minimization, we conducted MD for 10 ps at 0.1 K and then for 10 ps at 306 K with restraints of 1000 kJ/nm^2 on the protein heavy atoms to allow the solvent structure to accommodate the protein complex. Further equilibration of the

system for 200 ps at 306 K, using weaker restraints (10 kJ/nm) of the protein heavy atoms to their crystallographic positions, allowed distorted geometry and steric clashes in less well-determined regions of the protein to be relaxed.

MD and FEP Simulations. Following equilibration, we used a variety of MD-based simulations to explore the configurational landscape available to Bcu and the residues comprising the HBS. MD simulations were performed in an NVT ensemble with a cutoff of 12.0 Å for Coulombic interactions and 9.0 Å for van der Waals interactions. The pragmatic approach to the intractability of conducting simulations with infinite cutoffs is problematic and has led to differing approaches and recommendations. Cheatham et al.[30] recommended the use of particle mesh Ewald (PME) as being superior to a cutoff. However, Norberg and Nilsson point out these conclusions were drawn for a 9 Å cutoff and have shown results similar to those with PME[31] are obtained with conditions used here without the introduction of the artifactual infinite lattice Coulombic interactions of PME in a system designed to emulate solution conditions. The studies of binding of ligands to AR by Bisson et al.[32] were performed using conditions similar to ours but with a somewhat smaller cutoff of 9 Å. Nevertheless, this remains an open issue and is one of the reasons we have used multiple simulations and techniques. A time step of 2 fs was employed with a Nose-Hoover thermostat with a coupling parameter of 0.1.[27] After equilibration, the simulations were continued for 5.3 ns.

Slow Growth−Free Energy Perturbation. Although FEP theory has been used for calculation of the free energy of ligand binding, for this purpose it is valid for only small perturbations of ligand structure (e.g., a methyl group mutated to a chloride).[33,34] Instead, we have exploited it here to reduce the bias in ligand placement. In this protocol, the ligand is "grown slowly" in situ (by gradually turning on the nonbond potential). Our objective, rather that determining the binding free energy, is to allow time for the protein structure to adapt to the new ligand gently rather than creating a bias by "forcing" the insertion of the ligand into the 1T63 structure. This is accomplished according to the equation

$$E_{\mathrm{AR-Bcu}} = \lambda(E_{\mathrm{vdw}} + E_{\mathrm{coul}})_{\mathrm{AR-Bcu}}$$

where λ goes from 0 to 1.0 over 1000 ps.

The FEP stage was performed with a time step of 1 fs, and the nonbonded interactions between Bcu and AR were turned on continuously over a 1 ns interval by scaling λ linearly, from 0.0 to 1.0, while the temperature was linearly annealed from 0.1 to 306 K for the first 0.5 ns and then kept constant at 306 K for the final 0.5 ns of the FEP stage. Following this, the simulation was continued for 5 ns.

RESULTS AND DISCUSSION

Trajectories. To explore the structural details of the binding modes of bicalutamide in the AR LBD, we conducted a variety of MD-based simulations of the hydrated AR−Bcu complexes described in Materials and Methods. For comparison, we also simulated the AR complex with its endogenous ligand, dihydrotestosterone (DHT). The latter, along with a simulation of the experimentally determined AR W741L−Bcu construct in which Bcu is an agonist, not only provides a basis for understanding the perturbations induced by Bcu in the wild-type receptor but also, by comparison with the experimental structures, provides a benchmark for assessing the validity of the simulations and the significance of the antagonist-induced structural changes. The systems simulated, along with the nomenclature used to describe them, are listed in Table 1.

Table 1. Simulation Trajectories of AR−Ligand Complexes

name	system	initial ligand orientation	no. of runs
experimental structures			
sDHT	AR−DHT	AR−DHT	3
sBcuExp	AR W741L−Bcu	AR W741L−Bcu	3
antagonist complexes			
sBcu	AR−Bcu	AR W741L−Bcu	3
sBcuS1	AR−Bcu	AR−S1	3
sBcuFEP	AR−Bcu	AR W741L−Bcu	3

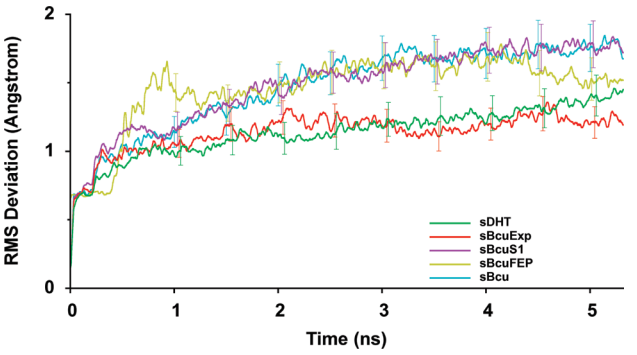

Figure 3. Plot of rmsd values of Cα atoms in the helical scaffold of the AR vs time for simulations of experimental and antagonist structures. Data for the experimental agonist complexes are colored green (sDHT) and red (sBcuExp). The trajectories for the antagonist structures are colored cyan (sBcu); those for the slow growth (FEP) simulation (sBcuFEP) are colored yellow and those for the structure in which the side chain conformations of key LBS residues were taken from the S1−AR complex (sBcuS1) magenta. Each curve is an average of three separate simulations with different initial velocities. The error bars indicate the standard deviation at that time of the three simulations.

The overall evolution of the AR structure in different complexes as well as an overall comparison with the experimentally determined structures may be obtained by plotting the root-mean-square deviation (rmsd) from the initial state for each complex. These trajectories are given in Figure 3. As one can see, the averaged trajectories of both experimentally determined complexes, WT AR−DHT (sDHT, green) and AR W741L−Bcu (sBcuExp, red), plateau at approximately the same rmsd values of ∼1 Å, showing good agreement with the experimental structures by this measure and as shown by the superpositions of the structures in Figure 4. On the other hand, the two trajectories of the WT AR complexes with Bcu, starting from the configurations of Bcu in the W741L and S1 complexes, both reflect significant distortions, exhibiting deviations from the agonist structures of ∼1.7 Å (cyan and magenta ligands, respectively). Of note is the behavior of the free energy perturbation simulations of the antagonist complex (sBcuFEP, yellow curve in Figure 3). Although initially the structure diverges dramatically from the agonist structure, it returns after 1 ns to follow the antagonist trajectories until 4 ns, at which time the deviation decreases and approaches that of the agonist structures.

A closer look at the three individual trajectories comprising the average of the FEP trajectories (not shown) reveals an intriguing behavior. Unlike the other trajectories, the individual FEP

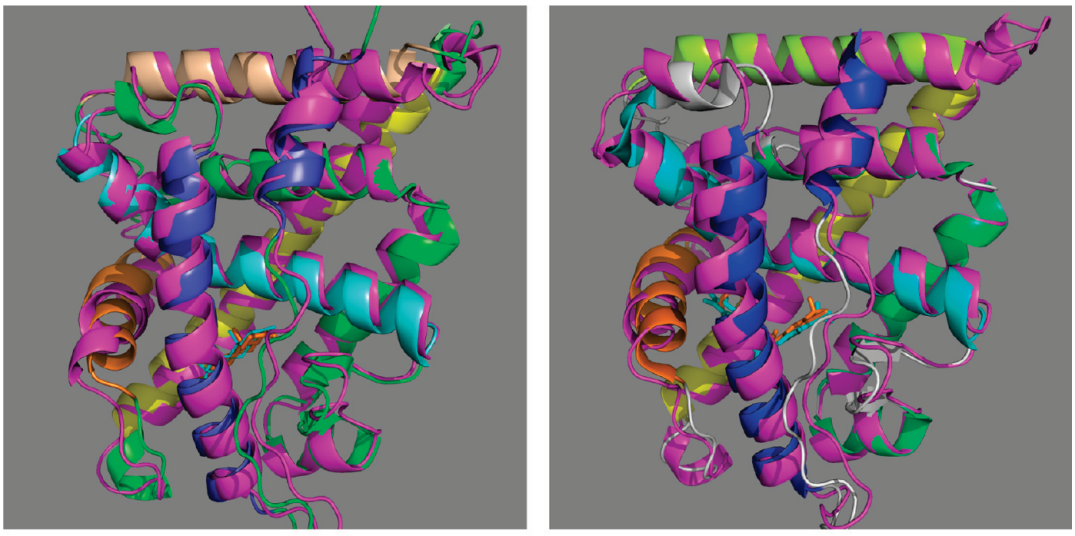

Figure 4. Superposition of the experimental (colored as in Figure 1) and simulated structures (colored magenta) of the AR−DHT (a) and AR W741L−Bcu (b) complexes. The helix scaffold Cα atom rmsd of these structures is slightly more than 1 Å, and as one can see from these figures, the overall AR structure, including the helical scaffold, is accurately recapitulated at this level. The ligands, DHT in panel a and Bcu in panel b, are shown as sticks (the experimental ligand structure is colored orange and the simulated configuration cyan).

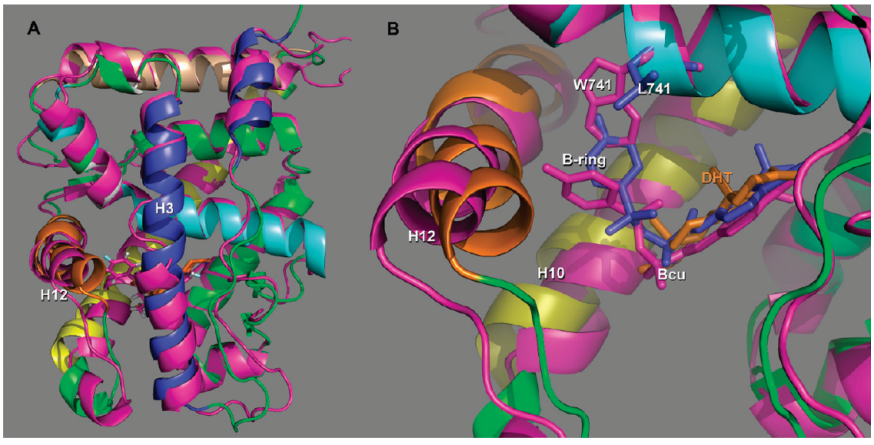

Figure 5. (A) Superposition of the 5 ns structure of the Bcu-bound AR (magenta) with the native AR−DHT complex (helices colored as in Figure 1). DHT and Bcu are shown as gold and magenta sticks, respectively. As one can see, Bcu induces global deformations in the AR structure, including some unraveling in the center of H3, and significant displacement of H12, both comprising components of the AF-2 site. (B) For this view, we removed H3 to better focus on the HBS. We have also depicted Bcu and L741 in the W741L mutant (both colored blue). The shift in the position of the B-ring of Bcu (magenta) by Trp741 is readily apparent when compared to its position when Leu is present at position 741 (blue). Again one can see the concomitant displacement of the key AF-2 helix H12 impairing the ability of the coactivator to bind at this site, consistent with the mechanism of antagonism in other NRs.

trajectories behave very differently. One of the trajectories essentially follows the path of the agonist trajectories of sDHT and sBcuExp, following a plateau with an rmsd of slightly more than 1 Å. The other two initially display large divergence from the initial structure (seen as the peak in sBcuFEP at ∼1 ns in Figure 3) and then after roughly 4 ns begin to converge back toward the agonist structure. The behavior of the trajectory following the agonist structures is unexpected, and we will return to the underlying structure of the complex below.

Mechanism of AR Antagonism by Bicalutamide. Structure of an AR−Antagonist Complex. The distortions underlying the deviations in the 5 ns trajectories of bicalutamide may be seen by superposing the 5 ns structure of the AR−Bcu (sBcu) complex on that of the AR−DHT complex (Figure 5). As one can see in these figures, the displacements in the AR induced by Bcu binding are not solely restricted to the region of the HBS but are also distributed throughout the receptor. Perhaps the most noteworthy distortion occurs in the helices comprising the AF-2 site. Here, there are distortions in all three helices forming the AF-2 site, H3, H4, and H12, with the largest displacement in H12 (Figure 5B). This is consistent with the theme of structural displacements underlying antagonism observed in other NRs.[1,2] A window into this mechanism has been provided by the naturally occurring W741L mutant.[24] The crystal structure of this complex demonstrated that indeed AR W741L adopted an agonist conformation upon binding to Bcu (rmsd from AR-DHT of 0.33).[25]

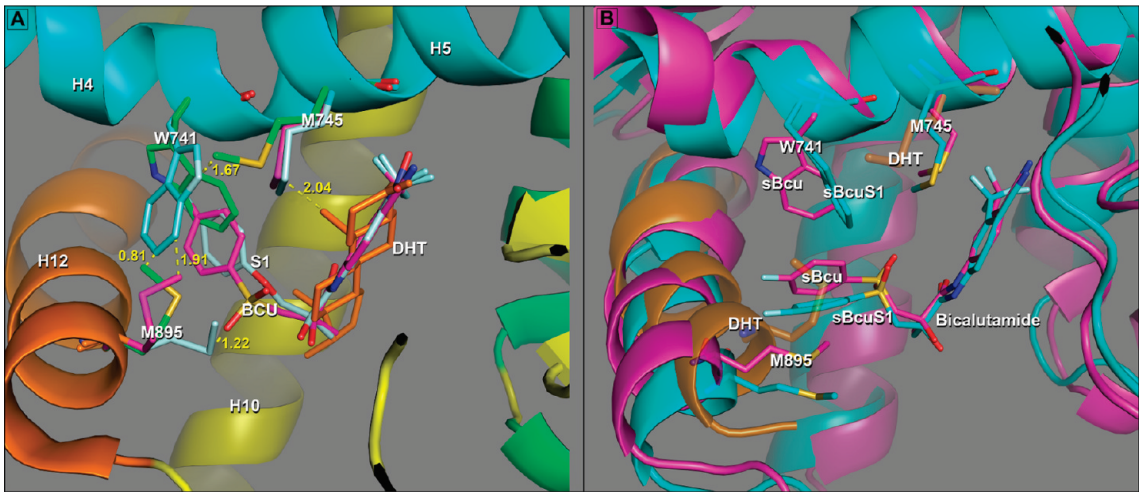

Figure 6. Adaptation of AR LBP to the B-ring of Bcu and S1 in experimental and simulated complexes. In both panels A and B, helix 3 is not displayed to provide an unobstructed view of binding pocket interactions. (A) The side chains can adapt to ligand in an agonist structure. Superposition of S1 (cyan), Bcu (magenta), and DHT (ligand colored gold and protein side chains colored green; H12 colored gold, H4 and H5 cyan, and H10 yellow) experimental AR structures. This figure shows the shift of M895 from its position in the DHT complex (green carbons), away from H12 toward the ether oxygen of S1 (cyan) to accommodate the repositioned W741. This S1 configuration does not accommodate Bcu in the agonist AR structure as when Bcu is bound, M895 in this position clashes with the sulfonyl group of Bcu. The orientation adopted by W741 in S1 to accommodate the B-ring brings it too close to the M745 side chain in DHT (green), and the configuration of M745 found in the S1 and Bcu complexes, which accommodates the rotated Trp741, is very close to the A-ring axial methyl group in DHT, thus being disallowed in the DHT complex. (B) The side chains are unable to adapt to ligand in an agonist structure. Superposition of the 5 ns structures for the sBcu simulation (magenta) and the sBcuS1 simulation (cyan). The semitransparent structure shows H12 and positions of M895 and M745 in the reference AR−DHT complex (gold). This shows the repositioning of the B-ring of Bcu "downward" and the concomitant displacement of H12 away from the LBS position, which creates an enlarged pocket to accommodate the shifted B-ring. Repositioning of the B-ring is accomplished primarily by a rotation about the C11−C13 bond from approximately −60° to 60°, while the A-ring occupies the identical position it occupies in the W741L X-ray structure (Figure 4b). The displacement of H12 allows M895 to adopt an extended conformation back into the LBS without clashing with the sulfonyl group of Bcu or with the B-ring of Bcu as seen in the colocation of M895 in the DHT complex (gold) and the B-rings of Bcu. This shift of H12 occurs in both trajectories as does the positioning of M745 into a space similar to that it occupies in the S1 and AR W741L crystal structures.

The structure revealed that the B-ring of Bcu occupied the cavity created by the absence of the Trp indole in the mutated complex,[25] while the A-ring is virtually in the same environment as the A-ring of DHT (Figure 5B). Thus, although a structural description of the AR antagonist mechanism still defied elucidation, this structure provided insight into possible interactions in the binding of Bcu to AR and along with MD allows for the description of one of the mechanisms by which Bcu antagonizes AR-dependent transcription. The MD studies of the WT AR−Bcu complex show that, as expected, W741 precludes the B-ring of Bcu from accessing that region of the HBS (Figure 5B). Instead, it is displaced "downward" toward H12, as seen from comparison of B-rings in the W741L mutant (blue) and the WT MD simulation (magenta). In the agonist conformation, this repositioning of the B-ring (magenta) would introduce several severe steric conflicts with M895 and I899 in helix 12 (e.g., I899 Cδ−C17, 2.02 Å; M895 Cα−F19, 2.24 Å), which, in turn, cause H12 to shift outward to accommodate the B-ring. We note that the A-ring pocket is basically conserved in the simulation, residing in essentially the same site that is occupied by the A-ring in the W741L complex and the DHT steroid hormone A-ring.

Some similar interactions were found by Bisson et al.[32] in their simulations of Bcu, although notable differences were observed as well. For example, the interactions between M895 and Bcu are observed in both results; on the other hand, interactions we observe with M745 are not mentioned in that study. The most significant difference, however, is the lack of perturbation of the position of H12 in their results. This may be due to the fact that they analyzed only a single simulation conducted over a shorter time frame (2.15 ns) with a shorter cutoff. It is possible that a combination of these factors prevented the propagation of perturbations induced by the ligand from reaching H12, though this is, of course, speculation.

Plasticity of the Hormone Binding Pocket: Determining Ligand Functionality. In Figure 6, we focus on the hormone binding site, to explore the detailed mechanism by which Bcu antagonizes the androgen response. Although the agonist activity of Bcu in the W741L mutant is fairly definitive in identifying W741 as playing a key role in the determination of a ligand's functional consequences (and therefore in future design efforts), it is not the sole determinant. This is demonstrated compellingly by the activity of the selective agonist S1 in the WT AR (Figure 2).[25] The substitution of an NO_2 at the para position on the A-ring is unlikely to be related to the agonist activity of S1 as many, if not most, antiandrogens have this functional group.[35] In addition, the B-ring is retained in S1. The result of structural studies, shown in Figure 6A, reveals how this is accomplished in the S1 complex but precluded with Bcu.[26]

The indole ring of W741 rotates away from H4 and toward H12. This creates a pocket into which the B-ring of S1 inserts. Perhaps not surprisingly, as seen in Figure 6A, it occupies essentially the same pocket inhabited by the B-ring of Bcu in the W741L construct, created by the Trp to Leu mutation.[25] The question of why W741 cannot adopt this configuration in the WT receptor to accommodate Bcu then arises. What emerges is a network of residues (M745-W741-M895) surrounding the B-ring pocket and adjacent to H12 that interact with the ligand and themselves. The degree to which this network can adapt in a

concerted fashion to a ligand without distorting the overall conformation of the receptor, and especially the position of H12, plays a major role in determining the functional consequences of a ligand occupying this pocket. Thus, the repositioning of Trp to accommodate the B-ring of S1 requires a concerted shift by M895 away from H12 and into the vicinity of the ether oxygen of S1 (cyan side chains in Figure 6A). This reorientation of M895 would be precluded by the sulfonyl group of Bcu in this configuration [$d(SO_2-S\delta) \sim 1.22$ Å (Figure 6A)]. We also note that the orientation adopted by W741 in the S1 complex is incompatible with the position of M745 (gold) in the DHT complex [$d(N\varepsilon-C\varepsilon) \sim 1.67$ Å]. Thus, the WT AR must find another way to accommodate Bcu, which leads to an antagonistic response.

We also note the configuration of M745 found in the AR−S1 (cyan) and AR W741L−Bcu (magenta) complexes that accommodates the rotation of Trp741 and is incompatible with the A-ring axial methyl group in DHT [$d(S\delta-C19 = 2.04$ Å]. Thus, we would surmise, for example, that a substitution on the A-ring of S1 occupying the C19 position of DHT might reposition M745, in turn forcing Trp back into the B-ring pocket and converting the S1 analogue into an antagonist much as the sulfonyl linkage in bicalutamide does acting through M895.

Conformational Response of the AR to Casodex: What Happens When the Network Cannot Accommodate the B-Ring in the Agonist AR Structure? In Figure 5, we show the overall distortion of AR engendered by binding of Bcu and compared it to the AR−DHT and AR W741L−Bcu complexes. Here we further focus our attention on the response to Bcu of the HBS residues and H12. To this end, the 5 ns structures starting with W741, M745, and M895 in their orientations in the DHT and S1 complexes, sBcu and sBcuS1, respectively, are shown in Figure 6B and compared to their configurations in the experimental structures. As one can see in this figure, the different trajectories result in the same overall deformation of the AR structure but differ somewhat in the details after 5 ns. This is to be expected of MD trajectories and is in fact why we assess multiple trajectories starting from different states and use different methodologies. The overall distortions result in expansion of the ligand binding pocket mainly by displacement of H12 from the ligand binding site (LBS), as the B-ring of Bcu is repositioned downward into the pocket created to accommodate it. As noted above, the repositioning of the B-ring brings it into the space occupied by M895 and I899 (not displayed) in the AR W741L−Bcu construct. The displacement of H12 and the concomitant reorientation and translation of M895 alleviate these clashes and allow M895 to adopt an extended conformation back into the LBS without clashing with the sulfonyl group of Bcu. This reorganization occurs in both trajectories, as does the positioning of M745 into a space similar to the one it occupies in the S1 and AR W741L structures. Of these three key residues, only the configuration of the Trp741 side chain differs somewhat in the two 5 ns structures.

A-Ring and Conserved Water Molecule. In contrast to the B-ring, the A-ring of Bcu occupies virtually the identical position in the HBS of WT AR in both simulations, sBcuS1 and sBcu, that it does in the W741L mutant. The A-ring sits in a hydrophobic pocket bound by helices H3 (L704 and L707), H5 (M745 and V746), H7 (M787), and H10 (L873) and strand β3 (F764) where it participates in the same interactions as in the W741L structure. The nature of the binding site and a subset of these interactions in the X-ray (W741L) and MD structure sBcuS1 are compared in Figure 7. As one can see, the interactions are highly conserved even though side chain conformations, such as M745, may be reoriented in some cases. In general, the corresponding interatomic distances in the two structures differ by only a few tenths of an angstrom. This binding mode of the A-ring appears to be highly favored, as in addition to the antagonist structures reported here X-ray structures indicate that the corresponding A-rings of essentially every ligand structure determined, including DHT (Figure 5B and ref 7), S1,[26] and R-3, an agonist that is an analogue of the antagonist hydroxyflutamide,[26] all lie in the same orientation in this pocket. In addition, the conserved water molecule found in the LBS of AR structures is also found in the Bcu antagonist structures at the same location. It should be pointed out that it was not placed there initially but rather emigrated from the initial, arbitrary position in which it was placed by the solvation procedure (see Materials and Methods).

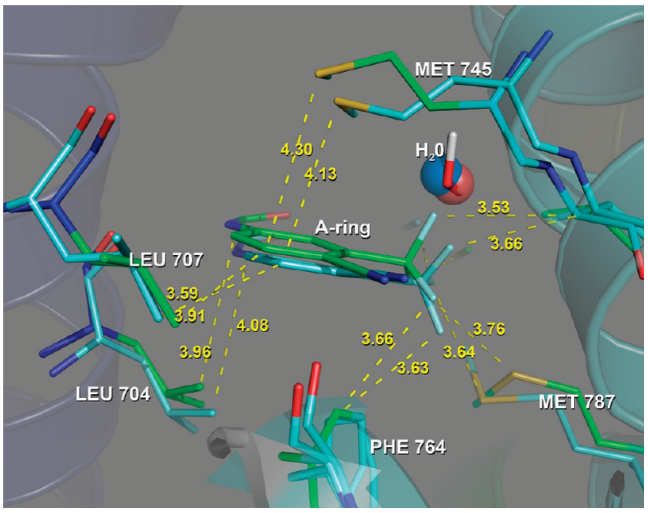

Figure 7. Superposition of the W741L experimental structure and WT AR−Bcu simulated structure showing the high degree of conservation of the A-ring pocket (Bcu is clipped at the amide attached to the A-ring). The A-ring in the experimental structure is shown with green carbons and the simulated structure with cyan carbons. The conserved water positions in the experimentally determined DHT and Bcu−AR W741L complexes are shown as blue and red spheres, respectively, while the stick model depicting the position from sBcuS1 shows simulated results account well for this interaction (the water position is similarly conserved in all simulated structures).

Free Energy Perturbation Results in an Intriguing Folded Conformation of Bcu. As noted above, the FEP trajectory of the Bcu−AR complex resembled those of the agonists more than those of the "standard" trajectories of Bcu. Inspection of the structure of the complex, given in Figure 8, shows why. As one can see, Bcu adopts an entirely different conformation, with the B-ring rotated and stacked in a compact folded structure over the A-ring (ball and stick, red carbons). The B-ring no longer extends into H12 and the AF-2 region as it does in structures obtained in the standard MD simulations (stick, cyan carbons) described above. As one can see, the A-ring position is still conserved, resulting in the folded structure occupying an expanded pocket enveloping the DHT site (shown as a transparent space-filling diagram). The elastic response of the receptor allows it to adapt to this Bcu conformation in an agonist-like conformation, with little distortion of helix H12 seen in the antagonist conformation. As one can see in Table 2, the displacements of the helices

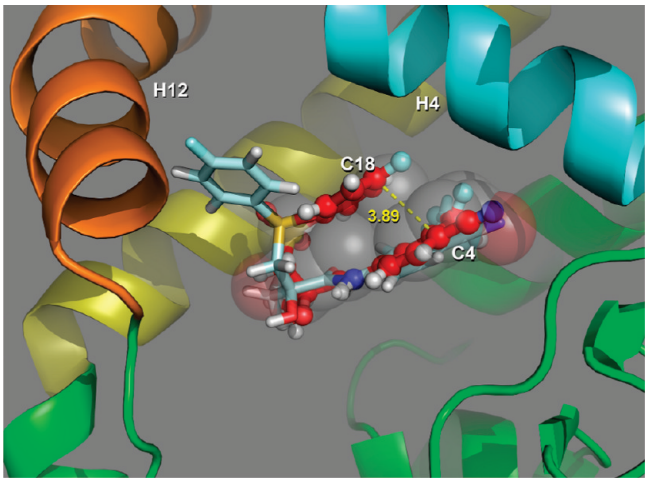

Figure 8. Free energy perturbation docking results in an unanticipated configuration and binding mode of bicalutamide. The folded configuration resulting from this slow growth procedure is shown as balls and sticks with red carbons. The extended configuration of Bcu is shown as sticks with cyan carbons. The DHT molecule is shown as a transparent space filling rendering. The FEP slow growth MD results in bicalutamide folding over into the pocket occupied by DHT, which expands somewhat to accommodate it. In this conformation, Bcu no longer sterically impacts H12 or the AF-2 site.

Table 2. Substructural Deviations from DHTexp (backbone)[a]

substructure	DHT5ns	BCU-FEP	BCUS1	BCU5ns
H3	1.19	1.28	1.63	1.64
H4	1.39	1.1	1.44	1.16
H5	0.87	0.67	0.92	1.23
H12	0.58	0.72	2.69	1.94
AF-2 site	1.15	1.11	1.81	1.52

[a] Structures superimposed fitting all backbone heavy atoms; the root-mean-square deviation (in angstroms) is computed for backbone heavy atoms of the substructures without further superimposition.

bordering the AF-2 site are significantly larger in the extended Bcu complexes as compared to the DHT or Bcu folded structure. This is especially true for H12 where the displacement is 3-fold greater in the former.

Energetic Analysis of Whether the Folded Ligand Conformation Is Plausible. To confirm that the conformational states of bicalutamide found in the MD simulations are energetically reasonable and not the result of a fortuitous rare statistical fluctuation, we have conducted high-level density functional QM calculations (DFT) of the conformational energetics of Bcu. The results are given in the first column of Table 3. Table 3 shows there are two equienergetic minima on the Bcu energy surface: an extended structure similar to that found in the W741L construct (and the two structures resulting from the standard MD simulations) and a stacked structure similar to that found bound to the AR in the FEP simulation (QMmin-Ext and QMmin-Folded, respectively). To assess the strain energies on binding, we minimized the energy of Bcu restrained to the bound configurations. As one can see, the induced strain energy is ~9 kcal for both conformational states, with the extended structures having slightly greater strain. On the basis of these results, the

Table 3. Binding and Strain Energies[a] of Agonist and Antagonist-like Bcu Conformations

AR−BCU complex	E_{strain} (QM)	$\langle E_{prot-lig} \rangle$	$E_{prot-lig}$(min)
QMmin-Folded	0.00		
QMmin-Ext	0.04		
5 ns	9.92	−45.76	−49.37
5 ns S1	9.89	−50.08	−49.26
5 ns FEP	8.53	−45.21	−48.28

[a] Energies in kilocalories per mole.

novel folded conformation of Bcu, stabilizing an agonist-like configuration of the AR−Bcu complex, is readily accessible.

Is the Binding Energy of the Folded Conformation of Bicalutamide Comparable to That of the Extended Structure? The question of the protein−ligand intermolecular energies for the different poses of Bcu then arises. Does the folded conformation induce significantly unfavorable interactions in the binding site, resulting in weaker binding? To address this question, we evaluated both the time-averaged and minimized binding energies of the three Bcu−AR complexes. These are given in the second and third columns of Table 3, respectively. Again, as one can see from these results, both the minimized and time-averaged binding energies are comparable, with the extended structures being slightly more favorable. The structure resulting from the initial S1 configuration is ~5 kcal/mol more favorable in the dynamically averaged calculation and ~1 kcal/mol in the minimized structures. Thus, both the strain and binding energy suggest that two distinct AR−Bcu complexes are accessible, an extended Bcu complex that significantly distorts the AF-2 pocket and the orientation of H12, accounting for its antagonist properties, and intriguingly a folded conformation that could be the species responsible for its agonist activity under increased AR expression levels or other agonist-producing environments.

SUMMARY

We have derived a structural model for an antagonist-bound conformation of the AR and the possible binding modes of bicalutamide, using MD and QM simulations, This provides a structural rationale for the antagonist activity of Bcu and a model for further design of AR modulators. Through an analysis of experimental and simulated structures, we have shown how a network of interacting side chains in the hormone binding site plays a key role in the functional consequences of agonist or antagonist activity and reorganizes when Bcu binds. As one might expect, a considerable shift in the position of H12 results from these interactions, resulting in distortion of the AF-2 coactivator binding site.

A slow growth procedure based on FEP methodology led to a novel docking pose for Bcu, a "folded" conformation with the A- and B-rings stacked. QM calculations for this folded configuration reveal that Bcu has two equienergetic minima: one similar to the "extended" conformation observed in the W741L structure and the two standard MD runs and the second analogous to the folded configuration resulting from the FEP simulation, suggesting the latter's accessibility. The docked folded conformation of Bcu has effects on the AR protein structure similar to those of the physiological agonist DHT and therefore could be responsible for the agonist activity of Bcu. In addition, it may provide a model for

the design of a new class of AR modulators, exploiting an expanded ligand binding cavity around the DHT site.

AUTHOR INFORMATION

Corresponding Author

*Department of Chemistry, University of Massachusetts, P.O. Box 310, Leverett, MA 01054. Phone: (619) 379-9768. Fax: (425) 696-7115. E-mail: athagler@gmail.com.

Funding Sources

This work was supported by National Institutes of Health Grant R43 CA132538 and National Science Foundation Grant CNS 0551500.

ACKNOWLEDGMENT

We thank Dr. Robert Fletterick and Dr. Sherin Abdul-Meguid for helpful comments on the manuscript.

ABBREVIATIONS

AR, androgen receptor; NR, nuclear receptor; Bcu, bicalutamide; T, testosterone; DHT, dihydrotestosterone; LBS, ligand binding site; WT, wild type; MD, molecular dynamics; QM, quantum mechanical; FEP, free energy perturbation; DFT, density functional theory; PC, prostate cancer; HBS, hormone binding site; sDHT, DHT simulation; sBcuExp, Bcu experimental simulation; sBcu, Bcu simulation; sBcuS1, Bcu S1 simulation; sBcuFEP, Bcu FEP simulation.

REFERENCES

(1) Gronemeyer, H., Gustafsson, J. A., and Laudet, V. (2004) Principles for modulation of the nuclear receptor superfamily. *Nat. Rev. Drug Discovery 3*, 950–964.

(2) Moore, J. T., Collins, J. L., and Pearce, K. H. (2006) The nuclear receptor superfamily and drug discovery. *ChemMedChem 1*, 504–523.

(3) Huggins, C. (1967) Endocrine-induced regression of cancers. *Science 156*, 1050–1054.

(4) Wirth, M. P., Hakenberg, O. W., and Froehner, M. (2007) Antiandrogens in the treatment of prostate cancer. *Eur. Urol. 51*, 306–314.

(5) Feldman, B. J., and Feldman, D. (2001) The development of androgen-independent prostate cancer. *Nat. Rev. 1*, 34–45.

(6) Matias, P. M., Donner, P., Coelho, R., Thomaz, M., Peixoto, C., Macedo, S., Otto, N., Joschko, S., Scholz, P., Wegg, A., Basler, S., Schafer, M., Egner, U., and Carrondo, M. A. (2000) Structural evidence for ligand specificity in the binding domain of the human androgen receptor. Implications for pathogenic gene mutations. *J. Biol. Chem. 275*, 26164–26171.

(7) Sack, J. S., Kish, K. F., Wang, C., Attar, R. M., Kiefer, S. E., An, Y., Wu, G. Y., Scheffler, J. E., Salvati, M. E., Krystek, S. R., Jr., Weinmann, R., and Einspahr, H. M. (2001) Crystallographic structures of the ligand-binding domains of the androgen receptor and its T877A mutant complexed with the natural agonist dihydrotestosterone. *Proc. Natl. Acad. Sci. U.S.A. 98*, 4904–4909.

(8) Hur, E., Pfaff, S. J., Payne, E. S., Gron, H., Buehrer, B. M., and Fletterick, R. J. (2004) Recognition and accommodation at the androgen receptor coactivator binding interface. *PLoS Biol. 2*, E274.

(9) Estebanez-Perpina, E., Moore, J. M., Mar, E., Delgado-Rodrigues, E., Nguyen, P., Baxter, J. D., Buehrer, B. M., Webb, P., Fletterick, R. J., and Guy, R. K. (2005) The molecular mechanisms of coactivator utilization in ligand-dependent transactivation by the androgen receptor. *J. Biol. Chem. 280*, 8060–8068.

(10) Ostrowski, J., Kuhns, J. E., Lupisella, J. A., Manfredi, M. C., Beehler, B. C., Krystek, S. R., Jr., Bi, Y., Sun, C., Seethala, R., Golla, R., Sleph, P. G., Fura, A., An, Y., Kish, K. F., Sack, J. S., Mookhtiar, K. A., Grover, G. J., and Hamann, L. G. (2007) Pharmacological and X-ray structural characterization of a novel selective androgen receptor modulator: Potent hyperanabolic stimulation of skeletal muscle with hypostimulation of prostate in rats. *Endocrinology 148*, 4–12.

(11) Baek, S. H., Ohgi, K. A., Nelson, C. A., Welsbie, D., Chen, C., Sawyers, C. L., Rose, D. W., and Rosenfeld, M. G. (2006) Ligand-specific allosteric regulation of coactivator functions of androgen receptor in prostate cancer cells. *Proc. Natl. Acad. Sci. U.S.A. 103*, 3100–3105.

(12) Chen, C. D., Welsbie, D. S., Tran, C., Baek, S. H., Chen, R., Vessella, R., Rosenfeld, M. G., and Sawyers, C. L. (2004) Molecular determinants of resistance to antiandrogen therapy. *Nat. Med. 10*, 33–39.

(13) Shen, M. M., and Abate-Shen, C. (2010) Molecular genetics of prostate cancer: New prospects for old challenges. *Genes Dev. 24*, 1967–2000.

(14) Burendahl, S., Treuter, E., and Nilsson, L. (2008) Molecular dynamics simulations of human LRH-1: The impact of ligand binding in a constitutively active nuclear receptor. *Biochemistry 47*, 5205–5215.

(15) Zhou, J., Liu, B., Geng, G., and Wu, J. H. (2010) Study of the impact of the T877A mutation on ligand-induced helix-12 positioning of the androgen receptor resulted in design and synthesis of novel antiandrogens. *Proteins 78*, 623–637.

(16) Quigley, C. A., De Bellis, A., Marschke, K. B., el-Awady, M. K., Wilson, E. M., and French, F. S. (1995) Androgen receptor defects: Historical, clinical, and molecular perspectives. *Endocr. Rev. 16*, 271–321.

(17) Wu, J. H., Gottlieb, B., Batist, G., Sulea, T., Purisima, E. O., Beitel, L. K., and Trifiro, M. (2003) Bridging structural biology and genetics by computational methods: An investigation into how the R774C mutation in the AR gene can result in complete androgen insensitivity syndrome. *Hum. Mutat. 22*, 465–475.

(18) Elhaji, Y. A., Stoica, I., Dennis, S., Purisima, E. O., Lumbroso, R., Beitel, L. K., and Trifiro, M. A. (2006) Impaired helix 12 dynamics due to proline 892 substitutions in the androgen receptor are associated with complete androgen insensitivity. *Hum. Mol. Genet. 15*, 921–931.

(19) Scher, H. I., Beer, T. M., Higano, C. S., Anand, A., Taplin, M. E., Efstathiou, E., Rathkopf, D., Shelkey, J., Yu, E. Y., Alumkal, J., Hung, D., Hirmand, M., Seely, L., Morris, M. J., Danila, D. C., Humm, J., Larson, S., Fleisher, M., and Sawyers, C. L. (2010) Antitumour activity of MDV3100 in castration-resistant prostate cancer: A phase 1−2 study. *Lancet 375*, 1437–1446.

(20) Chen, Y., Clegg, N. J., and Scher, H. I. (2009) Anti-androgens and androgen-depleting therapies in prostate cancer: New agents for an established target. *Lancet Oncol. 10*, 981–991.

(21) Tran, C., Ouk, S., Clegg, N. J., Chen, Y., Watson, P. A., Arora, V., Wongvipat, J., Smith-Jones, P. M., Yoo, D., Kwon, A., Wasielewska, T., Welsbie, D., Chen, C. D., Higano, C. S., Beer, T. M., Hung, D. T., Scher, H. I., Jung, M. E., and Sawyers, C. L. (2009) Development of a second-generation antiandrogen for treatment of advanced prostate cancer. *Science 324*, 787–790.

(22) Xiao, H. Y., Balog, A., Attar, R. M., Fairfax, D., Fleming, L. B., Holst, C. L., Martin, G. S., Rossiter, L. M., Chen, J., Cvjic, M. E., Dell-John, J., Geng, J., Gottardis, M. M., Han, W. C., Nation, A., Obermeier, M., Rizzo, C. A., Schweizer, L., Spires, T., Jr., Shan, W., Gavai, A., Salvati, M. E., and Vite, G. (2010) Design and synthesis of 4-[3,5-dioxo-11-oxa-4,9-diazatricyclo[5.3.1.0(2,6)]undec-4-yl]-2-trifluoro methyl-benzonitriles as androgen receptor antagonists. *Bioorg. Med. Chem. Lett. 20* 4491–4495.

(23) Attar, R. M., Jure-Kunkel, M., Balog, A., Cvijic, M. E., Dell-John, J., Rizzo, C. A., Schweizer, L., Spires, T. E., Platero, J. S., Obermeier, M., Shan, W., Salvati, M. E., Foster, W. R., Dinchuk, J., Chen, S. J., Vite, G., Kramer, R., and Gottardis, M. M. (2009) Discovery of BMS-641988, a novel and potent inhibitor of androgen receptor signaling for the treatment of prostate cancer. *Cancer Res. 69*, 6522–6530.

(24) Hara, T., Miyazaki, J., Araki, H., Yamaoka, M., Kanzaki, N., Kusaka, M., and Miyamoto, M. (2003) Novel mutations of androgen receptor: A possible mechanism of bicalutamide withdrawal syndrome. *Cancer Res. 63*, 149–153.

(25) Bohl, C. E., Gao, W., Miller, D. D., Bell, C. E., and Dalton, J. T. (2005) Structural basis for antagonism and resistance of bicalutamide in prostate cancer. *Proc. Natl. Acad. Sci. U.S.A. 102*, 6201–6206.

(26) Bohl, C. E., Miller, D. D., Chen, J., Bell, C. E., and Dalton, J. T. (2005) Structural basis for accommodation of nonsteroidal ligands in the androgen receptor. *J. Biol. Chem. 280*, 37747–37754.

(27) Van Der Spoel, D., Lindahl, E., Hess, B., Groenhof, G., Mark, A. E., and Berendsen, H. J. (2005) GROMACS: Fast, flexible, and free. *J. Comput. Chem. 26*, 1701–1718.

(28) Kitson, D. H., Avbelj, F., Moult, J., Nguyen, D. T., Mertz, J. E., Hadzi, D., and Hagler, A. T. (1993) On achieving better than 1-A accuracy in a simulation of a large protein: *Streptomyces griseus* protease A. *Proc. Natl. Acad. Sci. U.S.A. 90*, 8920–8924.

(29) Kaminski, G. A., Friesner, R. A., Tirado-Rives, J., and Jorgensen, W. L. (2001) Evaluation and Reparametrization of the OPLS-AA Force Field for Proteins via Comparison with Accurate Quantum Chemical Calculations on Peptides. *J. Phys. Chem. B 105*, 6474–6487.

(30) Cheatham, T. E., III, Miller, J. L., Fox, T., Darden, T. A., and Kollman, P. A. (1995) Molecular Dynamics Simulations on Solvated Biomolecular Systems: The Particle Mesh Ewald Method Leads to Stable Trajectories of DNA, RNA, and Proteins. *J. Am. Chem. Soc. 117*, 4193–4194.

(31) Norberg, J., and Nilsson, L. (2000) On the Truncation of Long-Range Electrostatic Interactions in DNA. *Biophys. J. 79*, 1537–1553.

(32) Bisson, W. H., Abagyan, R., and Cavasotto, C. N. (2008) Molecular basis of agonicity and antagonicity in the androgen receptor studied by molecular dynamics simulations. *J. Mol. Graphics Modell. 27*, 452–458.

(33) Simonson, T., Archontis, G., and Karplus, M. (1997) Continuum Treatment of Long-Range Interactions in Free Energy Calculations. Application to Protein-Ligand Binding. *J. Phys. Chem. B 101*, 8349–8362.

(34) Kollman, P. (1993) Free energy calculations: Applications to chemical and biochemical phenomena. *Chem. Rev. 93*, 2395–2417.

(35) Gao, W., Bohl, C. E., and Dalton, J. T. (2005) Chemistry and structural biology of androgen receptor. *Chem. Rev. 105*, 3352–3370.